engineering proceedings

MDPI

Proceeding Paper

Control of the Response to Water Vapor of Gas-Sensitive Zinc Oxide Nanostructures †

Svetlana S. Nalimova [1,*], Zamir V. Shomakhov [2], Vlada V. Miroshkina [1], Cong D. Bui [1] and Vyacheslav A. Moshnikov [1]

[1] Saint Petersburg Electrotechnical University "LETI", 197376, Russia; vladamiroshkina02@bk.ru (V.V.M.); congdoan6997@gmail.com (C.D.B.); vamoshnikov@mail.ru (V.A.M.)
[2] Kabardino-Balkarian State University, Chernyshevsky Street, 173, Nalchik, 360004, Russia; shozamir@yandex.ru
* Correspondence: sskarpova@list.ru
† Presented at The 11th International Electronic Conference on Sensors and Applications (ECSA-11), 26–28 November 2024; Available online: https://sciforum.net/event/ecsa-11.

Abstract: Gas-sensitive devices have great potential for use in a variety of applications, including environmental monitoring, medicine and industry. The stability of gas sensors based on zinc oxide can be significantly affected by the presence of water vapors in the atmosphere. Gas-sensitive layers based on ZnO nanowires were synthesized by hydrothermal method. The effect of different seed layers was studied in order to optimize the sensor properties of zinc oxide nanostructures. It was shown that layers consisting of zinc oxide nanowires synthesized using sacrificial doping on the seed layers of ZnO nanoparticles exhibited a moderate response to vapor of volatile organic compounds, with almost no response to water vapor.

Keywords: ZnO; ZnO-SiO_2; gas sensor; nanowires; sacrificial doping; humidity

Citation: Nalimova, S.S.; Shomakhov, Z.V.; Miroshkina, V.V.; Bui, C.D.; Moshnikov, V.A. Control of the Response to Water Vapor of Gas-Sensitive Zinc Oxide Nanostructures. *Eng. Proc.* **2024**, *5*, x. https://doi.org/10.3390/xxxxx

Academic Editor(s): Name

Published: 26 November 2024

1. Introduction

Gas-sensitive devices have a wide range of applications, including environmental monitoring, biomedical equipment and the pharmaceutical industry [1]. Their operation mechanism is based on the changing the electrical resistance of oxide materials when gas is absorbed onto the surface of a heated oxide [2]. Recently, zinc oxide nanostructures have been gaining attention as a promising material for highly sensitive and selective gas sensors [3]. ZnO has several advantages, including high biocompatibility, chemical stability, environmental safety, and low cost [4]. It can be used to detect various gases, such as hydrogen (H_2), ammonia (NH_3), methane (CH_4), carbon monoxide (CO), nitrogen dioxide (NO_2), ethanol, and acetone [5].

Depending on the synthesis method, zinc oxide forms a wide variety of crystalline structures, typically with a hexagonal wurtzite arrangement in which each oxygen (O^{2-}) ion is surrounded by four zinc (Zn^{2+}) ions at the vertices of a tetrahedron (Figure 1). This tetrahedral and non-centrosymmetric arrangement with polar symmetry along the hexagonal axis is responsible for the anisotropic growth of ZnO crystals [6]. This leads to a variety of nanostructure morphologies, including nanorods, nanowires, nanofibers, nanotubes, quantum dots, nanoparticles, nanofilms, and three-dimensional hierarchical structures [7].

One of the most significant factors influencing the characteristics of semiconductor gas sensors is the presence of water vapors, which can competitively adsorb on the surface of metal oxide structures. The effect of humidity on the response of TiO_2 nanowires to ethanol vapors was studied in [9]. Authors found that as humidity increased, the sensor response decreased by almost 100-fold. Among all possible defects in ZnO, oxygen

vacancies are crucial for enhancing the sensitivity of gas sensors [10,11]. In [12], it was demonstrated that zinc oxide nanorods with high oxygen vacancy content exhibit the highest response to ethanol vapor. An increased number of free electrons contribute to chemisorption of different oxygen particles, which participate in surface oxidation of ethanol. There are several approaches to escape the impact of humidity on the performance of semiconductor gas sensors. One of the simplest methods is surface treatment, which can be done by adding noble metals, alloying, modifying with hydrophobic materials, or combining with hydrophilic materials.

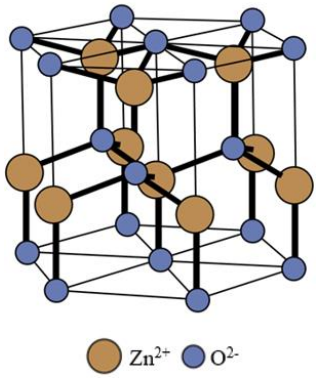

Figure 1. The crystal lattice of zinc oxide.

Subsequent processing of sensor materials can also improve their stability in humid environment. The proton beam surface treatment of zinc oxide (ZnO), described in [13], reduces response deviation when detecting nitrogen dioxide (NO_2) in a humid environment. This is due to the formation of vacancies in the ZnO structure, which have a higher adsorption energy for NO_2 molecules than for H_2O molecules. In addition, such processes as plasma fluorination of carbon nanotubes [14] and chemical etching [15] can also be used for processing. Water vapor exposure affects not only the baseline resistance and response of the gas sensor to the target gas, but also its response and recovery times. Humidity compensation can be achieved using mathematical models and neural networks to accurately calculate the concentration of the target gas.

In this paper, we have developed approaches to the synthesis of gas-sensitive zinc oxide layers that are resistant to the influence of water vapor. We have studied the influence of the seed layer type on the sensor properties of zinc oxide nanostructures.

2. Experiment

In this study, the synthesis of gas-sensitive ZnO layers consisted of two stages. First, a seed layer was deposited to substrates using the sol-gel method or precipitated from an aqueous solution of zinc salt. Finally, nanowires were grown using hydrothermal synthesis. The solutions were deposited on ceramic sensor platforms with gold electrodes in an interdigitated configuration [16]. The seed layer was prepared by sol-gel method using zinc nitrate hexahydrate ($Zn(NO_3)_2{\cdot}6H_2O$) and tetraethoxysilane (TEOS) [17–19]. Ethanol served as a solvent for the solutions. After dissolving the precursors in ethanol, the solution was deposited on the ceramic substrate by spin-coating. The substrate was then annealed at 350 °C for 30 min.

To form seed zinc oxide nanoparticles, five layers of an aqueous solution of zinc acetate dihydrate ($Zn(CH_3COO)_2{\cdot}2H_2O$) were applied to the sensor platform using spin-coating with subsequent annealing for 15 min at 500 °C. Zinc oxide nanowires were then formed on the seed layers through hydrothermal synthesis [20–23], which was carried out in an equimolar solutions of hexamethylenetetramine ($C_6H_{12}N_4$) and zinc nitrate hexahydrate ($Zn(NO_3)_2{\cdot}6H_2O$). Sodium iodide (NaI) or sodium bromide (NaBr) were added to the solutions to realize sacrificial doping. The corresponding samples were labeled as

ZnO(I) and ZnO(Br). The layers of ZnO nanowires was grown for one hour at 85 °C and were subsequently washed with distilled water before being annealed at 500 °C for 30 min.

The surface morphology of the seed layers and nanowire layers was analyzed using atomic force microscopy (AFM) and scanning electron microscopy (SEM). The sensor properties of synthesized nanostructures were studied. The experimental setup allows us to monitor the change in resistance of the sample as air and test gas are introduced in cell. The air flow passess through silica gel for dehumidification and split into two streams. The first stream of dry air is directed immediately towards the sample, while the second stream is saturated with vapors of studied substance, mixed with the dry air upon opening an electromechanical valve and introduced into the cell with a fixed sample. Measurements were taken at 250 °C. The test gases were isopropyl alcohol vapors at a concentration of 1000 ppm and water vapors at a concentration of 74,000 ppm. The graphs of the resistance dependence on time were build. To conduct a comparative analysis of the samples, the response values (S) to the vapors of the target gas were calculated as the ratios of the resistance of the gas-sensitive layer in air to its resistance in the presence of a given concentration of the target gas (vapors of isopropyl alcohol or water) in the atmosphere.

3. Results and Discussion

The AFM images of the synthesized seed layers are shown in Figure 1. As a result of sol-gel synthesis, porous net-like structures with a cross-section of branches in the micrometer range have been formed. Nanoparticles with sizes ranging from several hundred nanometers to 1 micrometer have been synthesized from an aqueous solution of a precursor salt. The results of the morphology study of the synthesized zinc oxide nanowires are shown in Figure 2. The diameter of the nanowires ranges from 20 to 120 nanometers, and the average length is approximately 200 nanometers.

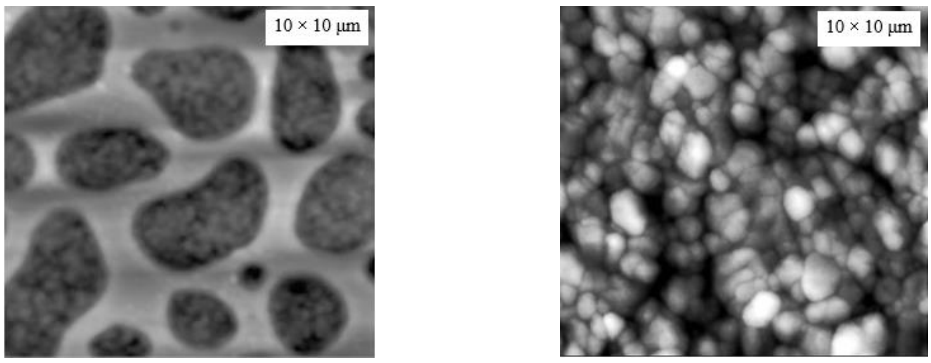

(**a**) (**b**)

Figure 1. Seed layers for hydrothermal growth of zinc oxide nanowires: (**a**) ZnO-SiO_2 nanocomposites, (**b**) ZnO nanoparticles.

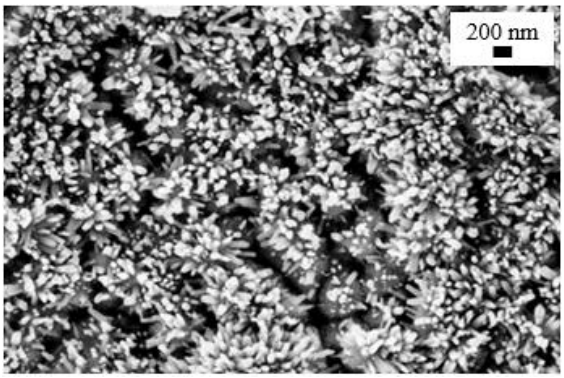

Figure 2. SEM image of a layer of ZnO nanowires [16].

As shown in our previous studies [16,21], the sacrificial doping of iodine and bromine leads to an increase in oxygen vacancies on the surface of zinc oxide nanowires. This, in turn, results in an increased gas-sensitive response.

The analysis of the interaction between samples of zinc oxide nanowires synthesized on different types of seed layers showed moderate response values shown in Table 1.

Table 1. Sensor responses of samples formed on different types of seed layers to vapors of isopropyl alcohol and water.

Seed Layer	Nanowires Type	$S(C_3H_7OH)$	$S(H_2O)$
ZnO-SiO_2 nanocomposites	ZnO(I)	1,58	1,84
	ZnO(Br)	1,67	2,17
ZnO nanoparticles	ZnO(I)	2,97	1,21
	ZnO(Br)	4,03	1,18

The gas-sensitive layers grown on ZnO-SiO_2 nanocomposites exhibit similar response values to water vapors and isopropyl alcohol vapors. This can be explained by the presence of silicon dioxide (SiO_2) fragments on the surface of the composites, which act as sites for the predominant adsorption of water molecules [24]. In this case, the ZnO-SiO_2 nanocomposite layer controls the flow of current through the sample. Changes in resistance occur due to changes in the thickness of conductive branches within the net-like structure, which is influenced by the Debye length. Under chosen conditions of sol-gel synthesis, branches with thicknesses ranging from hundreds of nanometers to micrometers are formed, resulting in moderate response values.

There are two mechanisms that can explain the effect of water vapors on the resistance of gas-sensitive layers. First, the adsorbed water vapors reduce the number of available adsorption sites, which in turn reduces the amount of oxygen that can be adsorbed on the surface of the semiconductor layer [25]. Second, the chemically adsorbed water molecule acts as a reducing agent and an electron donor, thereby reducing the baseline resistance of the sensor [26].

At the same time, the response of samples of zinc oxide nanowires synthesized on the seed layers of zinc oxide nanoparticles to isopropyl alcohol vapors significantly exceeds the response to water vapor. Moderate response values to isopropyl alcohol vapors may indicate that the current flows through the sample via a layer of seed ZnO nanoparticles. A high probability of this can be expected according to the results of the study on the morphology of the sample surface. The seed layer appears to have a large thickness, and the zinc oxide nanowires are not evenly distributed over the surface. Their length is also insufficient to form a continuous conductive network. A possible mechanism of the interaction between synthesized gas-sensitive layers and vapors of water and isopropyl alcohol is shown in Figure 3. When a gas-sensitive zinc oxide layer interacts with water vapor, adsorption occurs with the filling of oxygen vacancies on the surface. Nanowires can significantly increase the active area for water vapors adsorption, as they can act as "capture traps" for water molecules. However, when a current flows through the seed zinc oxide nanoparticle layer, the predominant adsorption of water vapors onto zinc oxide nanowires does not affect the resistance of gas-sensitive layer. When isopropyl alcohol vapors appear, adsorption occurs on the surface sites of the seed layer, and interaction with negatively charged oxygen reduces the resistance of the gas-sensitive layer.

By choosing the synthesis conditions such that the zinc oxide nanowires are loosely located on the substrate, it is possible to achieve an almost complete absence of response of these gas-sensitive materials to water vapors.

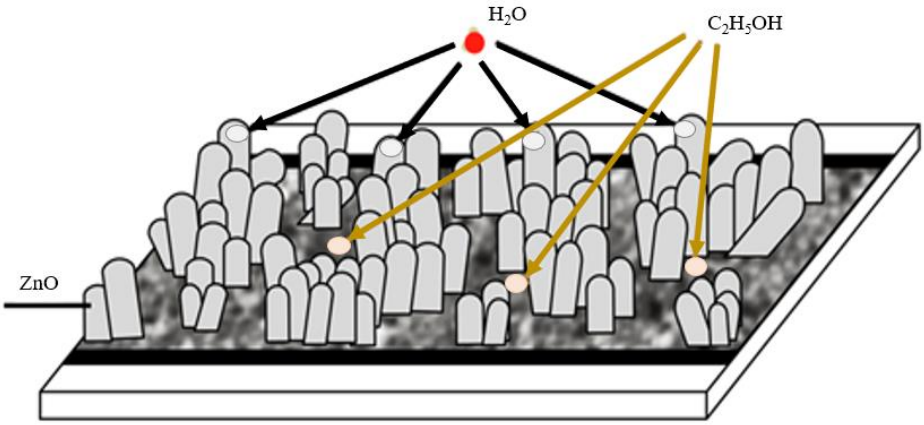

Figure 3. The mechanism of the interaction between the surface of zinc oxide nanostructures and gas molecules.

The negative effect of water vapors on the response of gas-sensitive layers may be caused by the formation of hydroxyl (OH) groups from adsorbed water molecules. Unlike conventional interfering gases, water molecules undergo a two-step adsorption process. As previously mentioned, water molecules are chemically adsorbed at the active sites of the gas-sensitive layer and reduced. After forming the first layer, as relative humidity increases, subsequent layers of water molecules physically adsorb [27]. Water molecules physically sorbed near the chemisorbed water layer can break down into H_3O^+ and OH^- ions due to the strong electrostatic field in the chemisorbed layer [28]. In physically adsorbed water, charge transfer occurs through proton jumping along a series of hydrogen bonds between ions and water molecules [29]. Such proton conductivity dominates over electric current and results in an increase in the conductivity of the sensitive layer and a reduction in its resistance as relative humidity increases.

Author Contributions: Conceptualization, V.M.; methodology, S.S.N. and Z.S.; validation, S.S.N. and V.M.; formal analysis, V.M.; investigation, V.M. and C.B.; writing—original draft preparation, S.S.N.; writing—review and editing, Z.V.S., V.M., C.D.B. and V.M. All authors have read and agreed to the published version of the manuscript.

Funding: This research received no external funding.

Institutional Review Board Statement: Not applicable.

Informed Consent Statement: Not applicable.

Data Availability Statement: Data are contained within the article.
Conflicts of Interest: The authors declare no conflicts of interest.

References

1. Panda, S.; Mehlawat, S.; Dhariwal, N.; Kumar, A.; Sanger, A. Comprehensive review on gas sensors: Unveiling recent developments and addressing challenges. *Mater. Sci. Eng.* **2024**, *308*, 117616. https://doi.org/10.1016/j.mseb.2024.117616.
2. Korotcenkov, G. Metal oxides for solid-state gas sensors: What determines our choice? *Mater. Sci. Eng.* **2007**, *139*, 1–23. https://doi.org/10.1016/j.mseb.2007.01.044.
3. Kumar, R.; Al-Dossary, O.; Kumar, G.; Umar, A. Zinc Oxide Nanostructures for NO_2 Gas–Sensor Applications: A Review. *Nano-Micro Lett.* **2015**, *7*, 97–120. https://doi.org/10.1007/s40820-014-0023-3.
4. Mandal, A.K.; Katuwal, S.; Tettey, F.; Gupta, A.; Bhattarai, S.; Jaisi, S.; Bhandari, D.P.; Shah, A.K.; Bhattarai, N.; Parajuli, N. Current Research on Zinc Oxide Nanoparticles: Synthesis, Characterization, and Biomedical Applications. *Nanomaterials* **2022**, *12*, 3066. https://doi.org/10.3390/nano12173066.
5. Franco, M.A.; Conti, P.P.; Andre, R.S.; Correa, D.S. A review on chemiresistive ZnO gas sensors. *Sens. Act. Rep.* **2022**, *4*, 100100. https://doi.org/10.1016/j.snr.2022.100100.
6. Kumar, R.; Kumar, G.; Umar, A. Zinc oxide nanomaterials for photocatalytic degradation of methyl orange: A review. *Nanosci. Nanotechnol. Lett.* **2014**, *6*, 631–650. https://doi.org/10.1166/nnl.2014.1879.

7. Gerbreders, V.; Krasovska, M.; Sledevskis, E.; Gerbreders, A.; Mihailova, I.; Tamanis, E.; Ogurcovs, A. Hydrothermal synthesis of ZnO nanostructures with controllable morphology change. *Cryst. Eng. Comm.* **2020**, *22*, 1346–1358. https://doi.org/10.1039/C9CE01556F.
8. Wang, Y.; Zhou, Y. Recent progress on anti-humidity strategies of chemiresistive gas sensors. *Materials* **2022**, *15*, 8728. https://doi.org/10.3390/ma15248728.
9. Shooshtari, M.; Salehi, A.; Vollebregt, S. Effect of temperature and humidity on the sensing performance of TiO_2 nanowire-based ethanol vapor sensors. *Nanotechnology* **2021**, *32*, 325501. https://doi.org/10.1088/1361-6528/abfd54.
10. Sun, K.; Zhan, G.; Zhang, L.; Wang, Z.; Lin, S. Highly sensitive NO_2 gas sensor based on ZnO nanoarray modulated by oxygen vacancy with Ce doping. *Sens. Act. B* **2023**, *379*, 133294. https://doi.org/10.1016/j.snb.2023.133294.
11. Kang, Y.; Yu, F.; Zhang, L.; Wang, W.; Chen, L.; Li, Y. Review of ZnO-based nanomaterials in gas sensors. *Solid State Ion.* **2021**, *116*, 115544. https://doi.org/10.1016/j.ssi.2020.115544.
12. Chang, C.M.; Hon, M.H.; Leu, I.C. Preparation of ZnO nanorod arrays with tailored defect-related characterisitcs and their effect on the ethanol gas sensing performance. *Sens. Act. B* **2010**, *151*, 15–20. https://doi.org/10.1016/j.snb.2010.09.072.
13. Bang, J.H.; Kwon, Y.J.; Lee, J.-H.; Mirzaei, A.; Lee, H.Y.; Choi, H.; Kim, S.S.; Jeong, Y.K.; Kim, H.W. Proton-beam engineered surface-point defects for highly sensitive and reliable NO_2 sensing under humid environments. *J. Hazard Mater.* **2021**, *416*, 125841. https://doi.org/10.1016/j.jhazmat.2021.125841.
14. Struzzi, C.; Scardamaglia, M.; Casanova-Chafer, J.; Calavia, R.; Colomer, J.-F.; Kondyurin, A.; Bilek, M.; Britun, N.; Snyders, R. Exploiting sensor geometry for enhanced gas sensing properties of fluorinated carbon nanotubes under humid environment. *Sens. Act. B* **2019**, *281*, 945–952. https://doi.org/10.1016/j.snb.2018.10.159.
15. Li, S.; Li, Z.; Zhang, M.; Wu, Z.; Kong, D.; Qian, H.; Sub, B. Etching process enhanced H_2O_2 sensing performance of SnO_2/Zn_2SnO_4 with reliable anti-humidity ability. *Anal. Methods* **2022**, *14*, 3335–3344. https://doi.org/10.1039/D2AY00573E.
16. Nalimova, S.; Shomakhov, Z.; Bobkov, A.; Moshnikov, V. Sacrificial Doping as an Approach to Controlling the Energy Properties of Adsorption Sites in Gas-Sensitive ZnO Nanowires. *Micro* **2023**, *3*, 591–601. https://doi.org/10.3390/micro3020040.
17. Nalimova, S.S.; Moshnikov, V.A.; Myakin, S.V. Controlling surface functional composition and improving the gas-sensing properties of metal oxide sensors by electron beam processing. *Glass Phys. Chem.* **2016**, *42*, 597–601. https://doi.org/10.1134/S108765961606017.
18. Bozhinova, A.S.; Kaneva, N.V.; Syuleiman, S.A.; Papazova, K.I.; Dimitrov, D.T.; Kononova, I.E.; Nalimova, S.S.; Moshnikov, V.A.; Terukov, E.I. Study of the photocatalytic and sensor properties of ZnO/SiO_2 nanocomposite layers. *Semiconductors* **2013**, *47*, 1636–1640. https://doi.org/10.1134/S106378261312004X.
19. Chudinova, G.K.; Nagovitsyn, I.A.; Gadzhiev, T.T.; Danilov, V.V.; Kurilkin, V.V.; Moshnikov, V.A.; Nalimova, S.S.; Kononova, I.E. Fluorescence of $ZnO:SiO_2$ and $SnO_2:SiO_2$ nanosized composite films under the action of human serum albumin. *Dokl. Phys. Chem.* **2014**, *456*, 74–76. https://doi.org/10.1134/S0012501614050030.
20. Nalimova, S.; Shomakhov, Z.; Moshnikov, V. Binary and Ternary Oxide Nanostructured Multisystems for Gas Sensors. *Eng. Proc.* **2023**, *48*, 47. https://doi.org/10.3390/ CSAC2023-14880.
21. Shomakhov, Z.V.; Nalimova, S.S.; Bobkov, A.A.; Moshnikov, V.A. X-ray photoelectron spectroscopy of the surface layers of faceted zinc-oxide nanorods. *Semiconductors* **2022**, *56*, 450–454. https://doi.org/10.1134/S1063782622130097.
22. Nalimova, S.S.; Shomakhov, Z.V.; Gerasimova, K.V.; Punegova, K.N.; Guketlov, A.M.; Kalmykov, R.M. Gas-sensitive composite nanostructures based on zinc oxide for detecting organic solvent vapors. *Phys. Chem. Asp. Study Clust. Nanostruct. Nanomater.* **2023**, *14*, 678–687. https://doi.org/10.26456/pcascnn/2022.14.678.
23. Nalimova, S.S.; Shomakhov, Z.V.; Kondratev, V.M.; Moshnikov, V.A.; Karmokov, A.M. Investigation of hierarchical gas-sensing $ZnFe_2O_4$ nanostructures. *J. Surf. Inv. X-Ray Synchrotron Neutron Tech.* **2023**, *17*, S416–S422. https://doi.org/10.1134/S1027451023070376.
24. Gulevich, D.; Rumyantseva, M.; Gerasimov, E.; Marikutsa, A.; Krivetskiy, V.; Shatalova, T.; Khmelevsky, N.; Gaskov, A. Nanocomposites SnO_2/SiO_2 for CO Gas Sensors: Microstructure and Reactivity in the Interaction with the Gas Phase. *Materials* **2019**, *12*, 1096. https://doi.org/10.3390/ma12071096.
25. Saruhan, B.; Lontio Fomekong, R.; Nahirniak, S. Influences of semiconductor metal oxide properties on gas sensing characteristics. *Front. Sens.* **2021**, *2*, 657931. https://doi.org/10.3389/fsens.2021.657931.
26. Jin, X.; Zha, L.; Wang, F.; Wang, Y.; Zhang, X. Fully integrated wearable humidity sensor for respiration monitoring. *Front. Bioeng. Biotechnol*. **2022**, *10*, 1070855. https://doi.org/10.3389/fbioe.2022.1070855.
27. Tsai, F.S.; Wang, S.J. Enhanced sensing performance of relative humidity sensors using laterally grown ZnO nanosheets. *Sens. Act. B* **2014**, *193*, 280–287. https://doi.org/10.1016/j.snb.2013.11.069.
28. Tai, W.P.; Oh, J.H. Humidity sensing behaviors of nanocrystalline Al-doped ZnO thin films prepared by sol–gel process. *J. Mater. Sci. Mater. Electron.* **2002**, *13*, 391–394. https://doi.org/10.1023/A:1016084309094.
29. Agmon, N. The grotthuss mechanism. *Chem. Phys. Lett.* **1995**, *244*, 456–462. https://doi.org/10.1016/0009-2614(95)00905-J.